

## Electrochemical Fabrication of Sandwich Nanostructures Based on Anodic Alumina

Zhao Jian Li and Ke Long Huang\*

*Institute of Functional Materials & Chemistry, College of Chemistry & Chemical Engineering,  
Central South University, Changsha 410083, PR China*

Este trabalho apresenta o projeto e a preparação bem sucedidos de um filme de alumina porosa anódica do tipo sanduíche (PAA/Al<sub>2</sub>O<sub>3</sub>/PAA). Utilizou-se o processo usual, em duas etapas, de anodização de ambos os lados de uma folha de alumínio. A estrutura do filme foi determinada por microscopia eletrônica de mapeamento e emissão de campo (SEM). Os resultados obtidos na microscopia SEM mostraram que as membranas PAA têm uma nano estrutura bem definida. Todos os nano buracos apresentaram-se de forma simétrica em ambos os lados da camada de barreira. O diâmetro médio do poro encontrado foi da ordem de 40 nm.

A sandwich porous anodic alumina (PAA/Al<sub>2</sub>O<sub>3</sub>/PAA) film was successfully designed and fabricated using the customary two-step anodization approach on both sides of an aluminum foil. The structure of the film was determined with field emission scanning electron microscopy (SEM). The SEM shows the PAA membranes has a well-defined nanostructure. All nanoholes stand symmetrically on both sides of the barrier layer. The average pore diameter reaches 40 nm.

**Keywords:** porous alumina membrane, anodization, template

### Introduction

The structure of porous anodic alumina (PAA) has been known as early as 1932<sup>1</sup> and it consists of an array of uniformly sized straight and parallel pores. Under appropriate anodic oxidation conditions, very regular self-ordered, honeycomb-like hexagonal arrays with a circular pore at the center of each hexagon can be obtained.<sup>2</sup> The pore diameters are tunable in the range of 4 to several hundred nanometers, making PAA an ideal template for creating arrays of nanostructured materials.<sup>3</sup> It has been explored as template growth of metallic nanowires,<sup>4-11</sup> semiconductor nanowires,<sup>12-15</sup> magnetic nanowires<sup>16</sup> or carbon nanotube.<sup>17,18</sup> However, all the above mentioned PAA membranes have only been formed on one side of the aluminum foil; the other side of the aluminum foil had to be removed. In contrast, if both sides of the aluminum foil are anodically oxidized to form two PAA membranes, a sandwich structure will be obtained. Peng and Chen<sup>19</sup> prepared a PAA/Al/PAA using two different anodic processes on each side of the aluminum foil. In this paper, the sandwich PAA/Al<sub>2</sub>O<sub>3</sub>/PAA membrane can be simply and rapidly fabricated by using the customary two-step oxidation process.

Here two graphite sheets are used as counter electrodes during the fabrication of PAA films. A schematic representation of the whole procedure is shown in Figure 1. In the first step, a clean aluminum sheet is anodically oxidized to form an alumina membrane (A) at 40 V and 15 °C in a solution of 0.3 mol L<sup>-1</sup> oxalic acid. This preformed membrane is subsequently removed by a phosphochromic acid solution to form a textured pattern of concave substrate (B) for the second anodic oxidation process. After another anodic oxidation of B under the same condition as the first step, a well-ordered PAA/Al<sub>2</sub>O<sub>3</sub>/PAA membrane (C) with

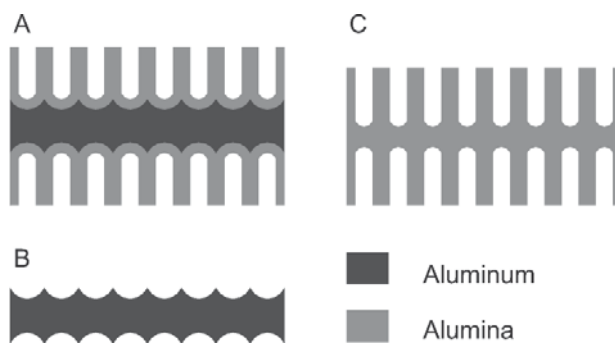


**Figure 1.** Schematic representation of the fabrication procedure for the formation of ordered porous alumina membrane. (A) Formation of the porous alumina layer after the first anodic oxidation process; (B) removal of the porous alumina layer; (C) formation of the sandwich porous anodic alumina (PAA/Al<sub>2</sub>O<sub>3</sub>/PAA) film after the second anodic oxidation process.

\*e-mail: klhuang@mail.csu.edu.cn; lizhaojian\_lzj@hotmail.com

ordered pores is formed. The two-step process results in a more ordered pore structure in the final template. Because pore formation begins at pits in the Al film, the initial pore structure is relatively disordered. As the anodization proceeds, the pore structure becomes more regular and the pore size distribution becomes more uniform. After first oxidation and removing the initial alumina film, the remained aluminum layer was textured with pits corresponding to the base of the pores from the first anodization step. The textured surface remained at the bottom of each curvature, where the resistance was the lowest and the electric field was the highest, so the pore nucleation was easier on a textured surface.<sup>20</sup> Then, a more uniform second alumina layer resulted.

## Experimental

In this work, the highly ordered hexagonal porous alumina membranes were prepared in oxalic acid *via* a two-step anodic oxidation process described as follows.<sup>2</sup> After being annealed at 500 °C for 23 h, a piece of high purity (20 × 20 mm, 75 μm thickness, 99.99%) aluminum foil was degreased in acetone by 300 s of ultrasonic cleaning. Then the sample was rinsed with distilled water and etched in 5 wt.% NaOH for 2 min. Electrodes made from these foils were electrochemically polished (5:1 v/v solution of EtOH/HClO<sub>4</sub>) at 6 °C for 1 min. Then, they were used as the central anodes in a home-made electrochemical cell, vertically suspended between two graphite sheets. A porous aluminum oxide was obtained at a constant voltage (40 V) in 0.3 mol L<sup>-1</sup> oxalic acid at 15 °C under continuous stirring.

The first anodic oxidation lasted 8 h and the second 24 h. After the first anodic oxidation, the strip-off process was carried out in a mixture solution (6 wt.% H<sub>3</sub>PO<sub>4</sub> + 1.8 wt.% H<sub>2</sub>CrO<sub>4</sub>) at 60 °C for 4 h. The exposed and well-ordered concave patterns on the aluminum substrate acted as self-assembled mask for the second anodic oxidation process (see Figure 1B). The transparent PAA/Al<sub>2</sub>O<sub>3</sub>/PAA film can be fabricated after the second anodic oxidation. The morphology and microstructure of the anodized samples were characterized using a scanning electron microscope (SEM, JSM-6700 F). The crystallographic structures of the samples were determined by X-ray powder diffraction (XRD) using a D/max 2550 X-ray diffractometer with Cu Kα radiation (λ=1.54056 Å).

## Results and Discussion

Figure 2 shows the variation of current densities with time throughout the process as described above. The

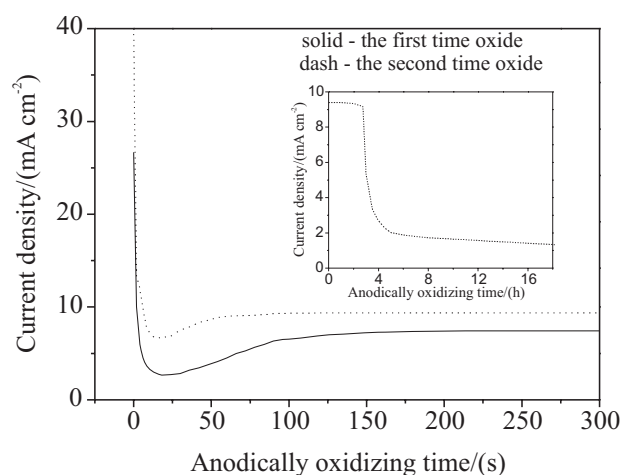


**Figure 2.** Current densities as a function of time during the anodic oxidation processes at 40 V in a solution of 0.3 mol L<sup>-1</sup> oxalic acid at 15 °C. The solid and dotted curves are for the first and second anodic oxidation processes, respectively.

solid and dash curves are for the first and second anodic oxidation processes, respectively. Two curves give detailed information of the oxidation process for the preparation of sandwich PAA/Al<sub>2</sub>O<sub>3</sub>/PAA membrane. The current *vs.* time curve appears to be similar to typical aluminum oxidation plots reported elsewhere in the literature,<sup>20</sup> where, our plots exhibit the same dramatic drops and rises of the current, followed by a current plateau corresponding to a constant anodic oxidation of the aluminum. The *I-t* curve shows the growth of porous layers in this solution undergo three stages during anodizing.

In the initial stage, a sudden decrease of the current means the aluminum oxide begins growing. Secondly, nanopores start to form and, after about 100 s, the current becomes stable and steady state pore grows.

After first oxidation and removing the initial alumina film, there were textured with pits on both sides of the remained aluminum layer. The time for pore nucleation and growth for the second oxidation process is shorter than those in the first oxidation process. Two graphite electrodes are used to accelerate the dissolution of aluminum substrate. After approximately 3 h in the second anodic oxidation, the current decrease and then become stable (see the inset of Figure 2). With the localized pore growth and the local dissolution process, resistance of the electrode increases continuously resulting in a slow decrease in current. When the current drops to a minimum, the formation rate of the oxide is equal to the local dissolution rate of the oxide barrier layer at the bottom of the pores. The anodic oxidation reaches a new balance; accordingly, the apparent current reaches a constant value.

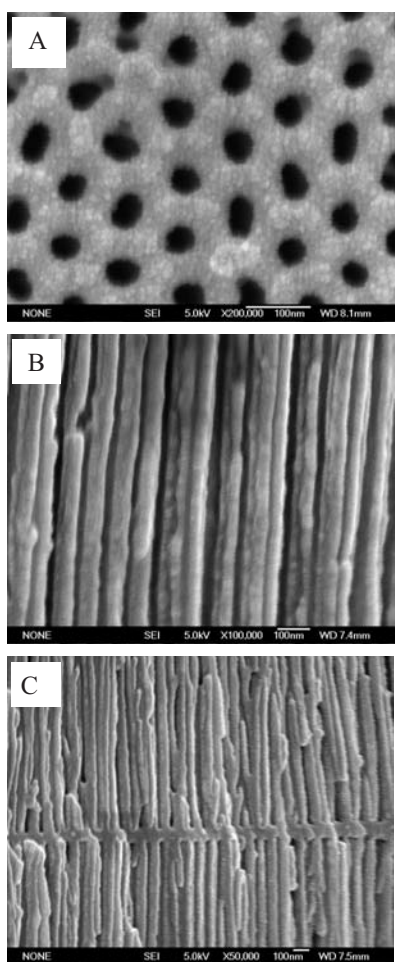


**Figure 3.** SEM images of anodic alumina films after the second anodization at 40 V in 0.3 mol L<sup>-1</sup> oxalic acid at 15 °C. (A) Top surface; (B) and (C) Cross-section surface.

Figure 3 shows the SEM images of top surface (Figure 3A) and cross-section surface (Figure 3B and 3C) of PAA after the second anodic oxidation. From Figure 3A, it can be seen that circular pores are uniformly distributed on the surface. The average pore diameter reaches 40 nm. The cross section image of Figure 3B shows the parallel alignment of the pores, with the same diameter as Figure 3A. Figure 3C shows the bottom configuration of the pores, which are not uniform like the top hole and have some branches. Two pore bottoms are connected by an oxide layer, the so-called “barrier layer”. The thickness of the barrier layer is ~100 nm matching case the anodizing ratio (the thickness of barrier oxide layer to dc voltage) of 1.4 nm/V determined.<sup>21</sup> The thickness of the as-fabricated PAA/Al<sub>2</sub>O<sub>3</sub>/PAA film is ~45 μm. The above results show that the fabricated PAA/Al<sub>2</sub>O<sub>3</sub>/PAA sandwich has a well-defined nanostructure.

Moreover, the as-prepared sample is shown to be amorphous in nature (Figure 4), as observed by using the XRD technique.

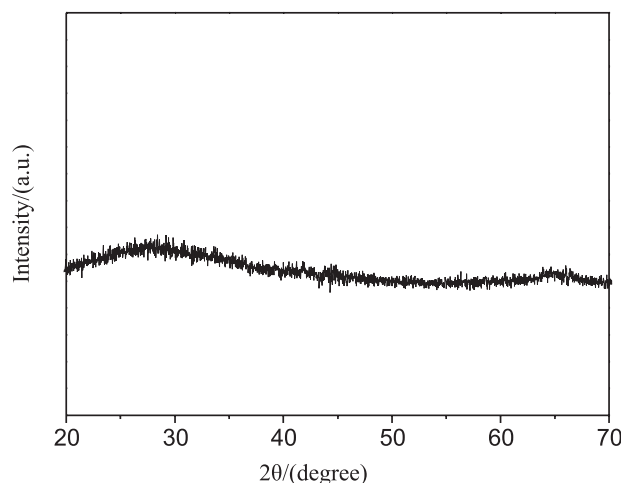


**Figure 4.** The XRD pattern of the as-prepared sample.

## Conclusions

The sandwich porous anodic alumina membranes (PAA/Al<sub>2</sub>O<sub>3</sub>/PAA) can be simply and rapidly fabricated from aluminum foil through a two-step oxidation process. The current vs. time curve appears to be similar to typical aluminum oxidation plots. The SEM images show that the fabricated PAA/Al<sub>2</sub>O<sub>3</sub>/PAA sandwiches have well-defined nanostructures. Pore diameter of ~40 nm and barrier layer thickness of ~100 nm can be achieved easily using the present fabrication procedure. The designed PAA/Al<sub>2</sub>O<sub>3</sub>/PAA sandwich nanostructures provide more research and application opportunities for nanoscience and nanotechnology. For example, they can serve as templates to prepare complicated nanostructured sandwiches as well as nanowires.

## Acknowledgment

This work was supported by Natural Science Foundation of Hunan Province of P. R. China (Grant No. 02JJY3044).

## References

1. Setch, S.; Miyata, A.; *Sci. Pap. Inst. Phys. Chem. Res. (Tokyo)* **1932**, *19*, 237.
2. Masuda, H.; Fukuda K.; *Science* **1995**, *268*, 1466.
3. Cojocaru, C. S.; Padovani, J. M.; Wade, T.; Mandoli, C.; Jaskierowicz, G.; Wegrowe, J. E.; Morral, A. F. I.; Pribat, D.; *Nano. Lett.* **2005**, *5*, 675.
4. Pang, Y. T.; Meng, G. W.; Zhang, Y.; Fang, Q.; Zhang, L. D.; *Appl. Phys. A* **2003**, *76*, 533.
5. Gao, T.; Meng, G. W.; Zhang, J.; Wang, Y. W.; Liang, C. H.; Fan, J. C.; Zhang, L. D.; *Appl. Phys. A* **2001**, *73*, 251.

6. Pang, Y. T.; Meng, G. W.; Shan, W. J.; Zhang, L. D.; Gao, X. Y.; Zhao, A. W.; Mao, Y. Q. *Appl. Phys. A* **2003**, *77*, 717.
7. Li, L.; Zhang, Y.; Li, G. H.; Song, W. H.; Zhang, L. D.; *Appl. Phys. A* **2004**, *00*, 1.
8. Wu, M. T.; Leu, I. C.; Yen, J. H.; Hon, M. H.; *J. Phys. Chem. B* **2005**, *109*, 9575.
9. Chu, S. Z.; Wada, K.; Inoue, S.; Todoroki, S. I.; *Chem. Mater.* **2002**, *14*, 4595.
10. Chu, S. Z.; Inoue, S.; Wada, K.; Kurashima, K.; *J. Phys. Chem. B* **2004**, *108*, 5582.
11. Sander, M. S.; Gronsky, R.; Sands, T.; Stacy, A. M.; *Chem. Mater.* **2003**, *15*, 335.
12. Zheng, M. J.; Li, G. H.; Zhang, X. Y.; Huang, S. Y.; Lei, Y.; Zhang, L. D.; *Chem. Mater.* **2001**, *13*, 3859.
13. Goh, C.; Coakley, K. M.; McGehee, M. D.; *Nano. Lett.* **2005**, *5*, 1545.
14. Hultheen, J. C.; Martin, C. R.; *J. Mater. Chem.* **1997**, *7*, 1075.
15. Jiang, K. Y.; Wang, Y.; Dong, J. Y.; Gui, L. L.; Tang, Y. Q.; *Langmuir* **2001**, *17*, 3635.
16. Ji, G. B.; Tang, S. L.; Gu, B. X.; Du, Y. W.; *J. Phys. Chem. B* **2004**, *108*, 8862.
17. Suh, J. S.; Lee, J. S.; *Appl. Phys. Lett.* **1999**, *75*, 2047.
18. Hu, W. C.; Gong, D. W.; Chen, Z.; *Appl. Phys. Lett.* **2001**, *79*, 3083.
19. Peng, X. S.; Chen, A. C.; *Nanotechnology* **2004**, *15*, 743.
20. Yuan, J. H.; He, F. Y.; Sun, D. C.; Xia, X. H.; *Chem. Mater.* **2004**, *16*, 1841.
21. Brevnov, D. A.; Rama Rao, G. V.; López, G. P.; Atanassov, P. B.; *Electrochim. Acta* **2004**, *49*, 2487.

Received: July 10, 2006

Web Release Date: March 30, 2007